

## Ground motion simulations

During the project there have been conducted ground motion simulations for nine different earthquake scenarios on various faults in the area around Izmir. The technique adopted for these calculations is a hybrid broad-band ground motion simulation technique, which have been previously validated in other areas, (Pulido and Kubo, 2004; Pulido et al., 2004; Sørensen et al., 2007). The earthquake scenarios conducted during this project are based on already existing knowledge for source parameters, local as well as regional, which was found during comprehensive literature search.

## Fault rupture scenarios

The faults for which there have been conducted ground motion simulations on are previously recognized by the Mineral Research and Exploration Institute of Ankara, Turkey, (MTA), (Emre et al., 2005b), and a figure showing the area near Izmir and the scenario faults (simplifications of the faults mapped by Emre et al.) is given in figure 1.

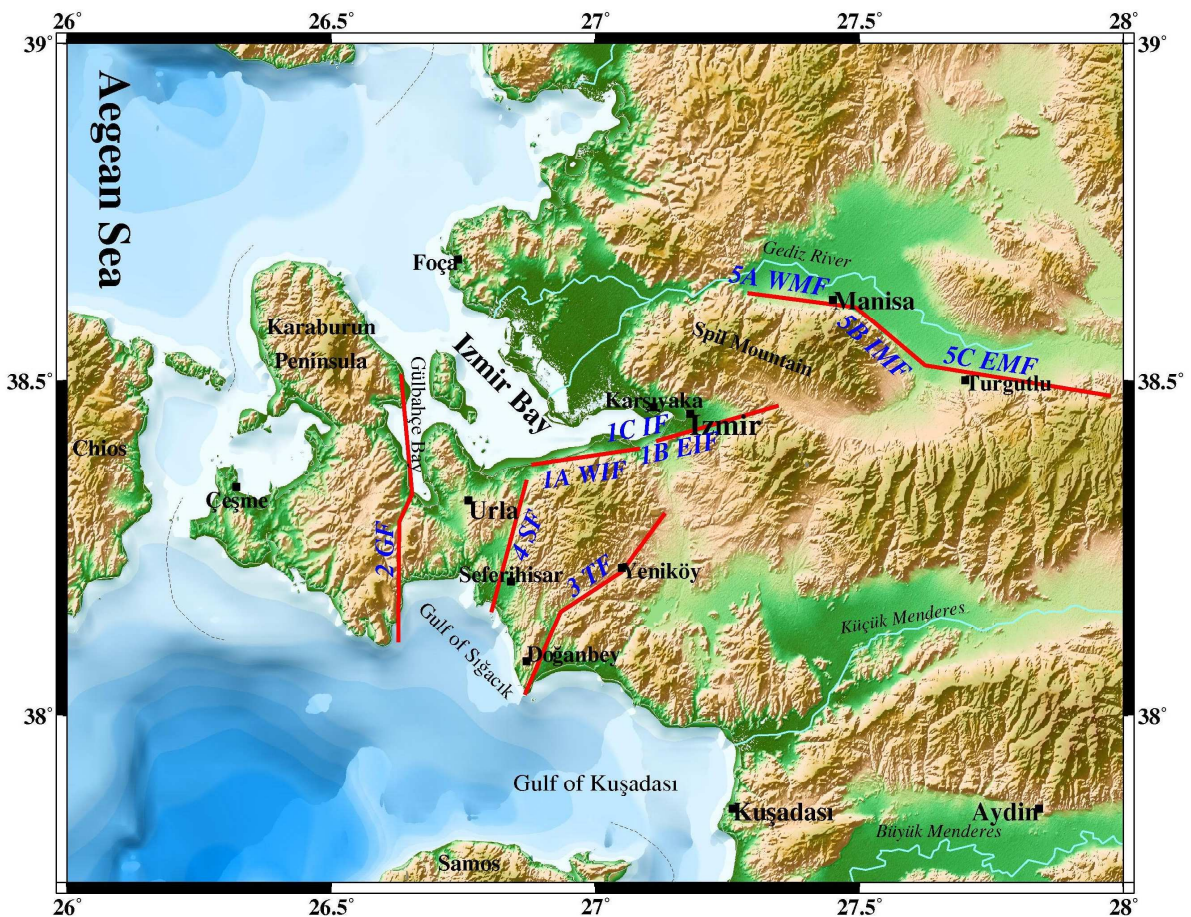


Figure 1: Map showing the simplified faults for which there have been conducted ground motion simulations for in this study. The code for the different scenarios is written in blue next to the respective faults. Scenario 1C IF is a combined rupture of fault segments 1A WIF and 1B EIF, with a 3 kilometer step-over in the central part of the fault.

The different faults are described shortly in the following.

- Izmir fault (scenario 1A WIF, 1B EIF and 1C IF) is a tow segmented normal fault that crosses underneath the metropolitan area of Izmir. The fault is believed to have caused the most destructive earthquake in the area in time, with a magnitude 6.8 earthquake in 1688, (Ambraseys and Finkel, 1995). In instrumental time there have occurred two earthquake of magnitude 5.5 and 5.3 in 1977 and 1979 respectively, (Emre et al., 2005b). There have in the project been calculated three different earthquake scenarios to occur in the Izmir fault; a rupture on the western segment (1A WIF), a rupture on the eastern segment (1B EIF) and a combined rupture of both segments with a small step-over in between (1C IF).
- Gülbahçe fault (scenario 2 GF) is a three segmented left lateral strike-slip fault striking almost north-south along the peninsula west of Izmir. This fault ends in the south in Gulf of Siğacik where there in 2005 was observed an earthquake swarm and as late as in February 2008 there is observed activity in the north of this fault. On this fault there is conducted one earthquake scenario, where the entire fault breaks, with a hypocenter located in the south near the earthquake activity from 2005, (Emre et al., 2005a).
- Tuzla fault (scenario 3 TF) is also a three segmented right lateral strike-slip fault. This fault is striking from Değanbey in south-west to just south of Izmir in north-east. This fault is not clearly visible on the surface. In 1992 there was recorded a magnitude 6.0 event on this fault, (Emre et al., 2005b). The hypocenter of this scenario earthquake was placed in the south in order to produce a directivity effect toward Izmir, and thereby creating the worst case scenario for Izmir, when it come to a rupture on this fault.
- Seferihisar fault (scenario 4 SF) is a right lateral strike-slip fault located between the Gülbahçe and Tuzla faults with an orientation from south-west to north-east ending near the most western segment of the Izmir fault. There has been ruptures on the faults in recent time, as in april 2003, where there occurred 2 events of magnitude 5.2 and 5.7 within few days, (Benetatos et al., 2006; Larson, 2006)
- Manisa fault (scenario 5A WMF, 5B IMF and 5C EMF) is a large normal fault that is located north-east of Izmir. The fault consists of several segments, and in this project there have been conducted ground motion simulations on three of these segments

(western, intermediate and eastern segments). There have not been made a combined rupture of the segments (as was the case of the Izmir fault), due to the large deviation in strike along the different fault segments and the bends separating the segments are assumed to be too large to let the rupture propagate. The fault is known to have produced significant earthquakes in historic times like the M=6.7 event in 1845 and the fault activity was also manifested in 1994 by an M=5.2 earthquake, (Emre et al., 2005b; Papazachos and Papazachou, 1997).

### **Ground motion simulation results**

For each of the nine earthquake scenarios there have been calculated waveforms for a grid of simulation points covering the study area of longitude 25.4°-29.0°E and latitude 37.0°-39,8°N, approximately covering an area of radius 150 km from Izmir. All the calculations are done for bedrock conditions, and of this reason there have not been taken local site effects (sediment layers, slope instabilities etc.) into account.

The areal distribution of the peak ground motions (peak ground acceleration, PGA, and velocity, PGV) for each scenario are plotted in separate maps, by extracting the peak motions for each simulation points. There were also calculated waveforms for each scenario in both acceleration and velocity for a station located in the center of Izmir. There calculated ground motions for all the scenario earthquakes have been compared with existing empirical attenuation relations, local as well as world-wide. Finally the frequency response spectra for each earthquake scenario have been calculated.

### Ground motion distribution

The ground motion distributions for all nine earthquake scenarios are shown in figure 2-4. It is evident that the most significant peak ground motions for each earthquake scenario are located above the ruptured fault plane.

There are for the scenario earthquakes for the strike-slip events (scenario 2 GF, 3 TF and 4 SF) in figure 3 are observed a more prominent directivity effect along the fault rupture than in the simulated normal fault events on Izmir and Manisa faults in figure 2 and 4. Especially is the effect of rupture directivity observed for the scenario earthquakes on Gülbahçe and Tuzla faults. That the directivity effect is not clearly observed on the Seferihisar fault (figure 3e and f) can be due to even though this fault is a strike-slip fault it has a relatively large normal component, whereas the earthquake focal mechanisms on both Gülbahçe and Tuzla faults are of more pure strike-slip mechanisms.

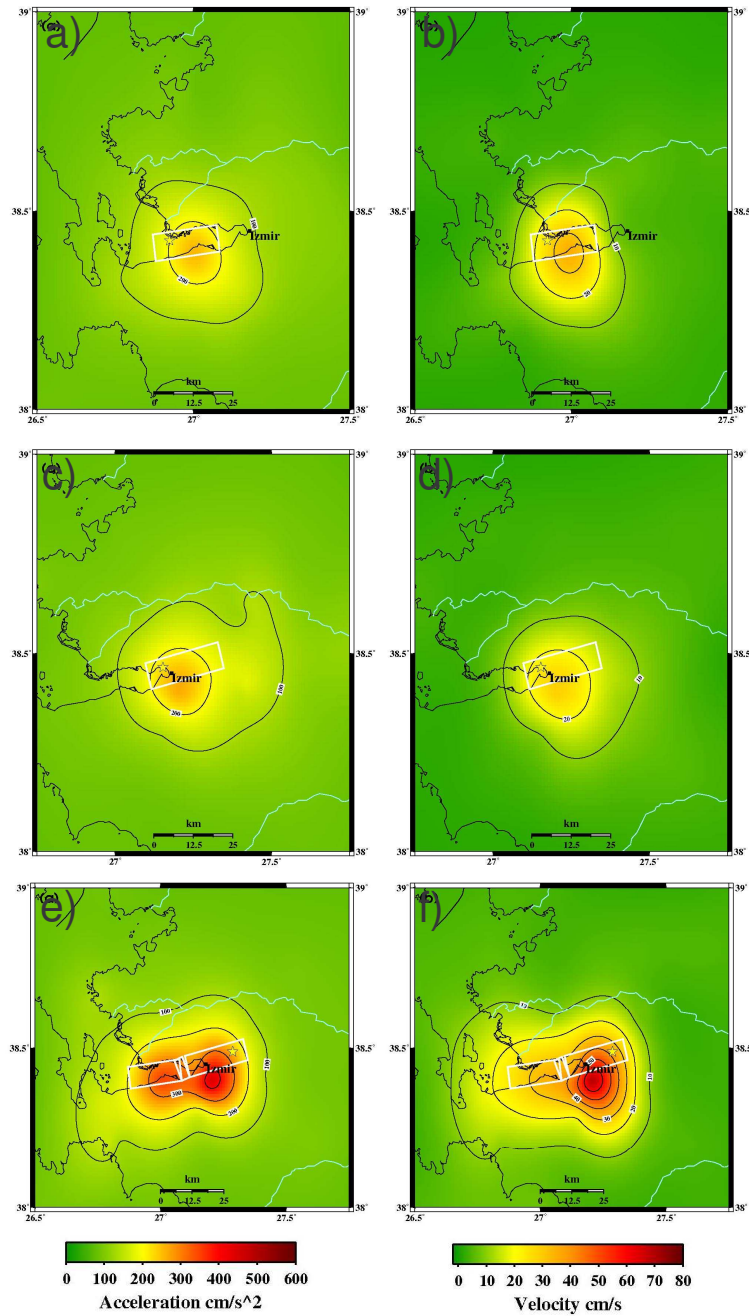


Figure 2: Peak ground motions for the three scenario earthquakes on the Izmir fault. The ruptured fault planes are sketched as white boxes and the epicenter for each scenario are marked with a yellow star. To the left (a, c and e) are shown the peak ground acceleration (PGA), the contour colors are from 0-600  $\text{cm/s}^2$ . In the maps to the right (b, d and f) are shown the peak ground velocity (PGV), the contour colors are from 0-80  $\text{cm/s}$ . The maps in a) and b) shows the peak ground motion distribution for the earthquake scenario of the western segment on the Izmir fault (scenario 1A WIF), c) and d) is for the earthquake scenario on the eastern segment of the Izmir fault (scenario 1B EIF) and e) and f) is for the earthquake scenario of the combined rupture of the western and eastern segment of the Izmir fault (scenario 1C IF).

Comparing the different maps showing peak ground motion distributions for the nine earthquake scenarios, it is evident that the earthquake scenario on Gulbahçe and Tuzla faults produces the largest peak ground accelerations, with maximum acceleration values near  $600\text{cm/s}^2$ . Whereas the scenario earthquake of the entire Izmir fault produces the largest peak ground velocities, with a maximum velocity value of approximately  $70\text{ cm/s}$ . It is

seen that the largest ground motions in the center of Izmir (inner part of the Izmir bay) is produced by the scenario earthquake on the entire Izmir fault (1C IF). In both this earthquake scenario and the scenario on the eastern part of the Izmir fault, the rupture occurs on a fault underlying the central part of Izmir, and the high values of peak ground motions observed in the center of Izmir for these two scenarios are partly explained from the proximity of the site to the scenario faults. Because of the short distance the effect of attenuation is a minimum.

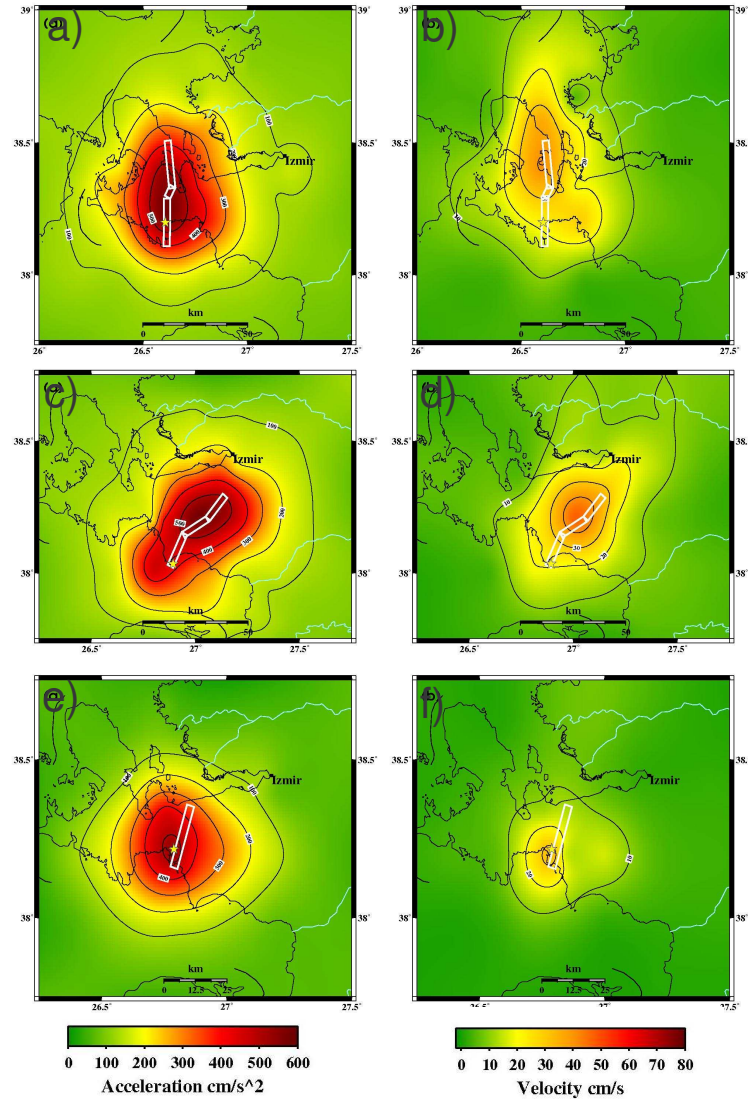


Figure 3: Peak ground motions for the scenario earthquakes on the Glbahe fault (scenario 2 GF), (a and b), Tuzla fault (scenario 3 TF), (c and d) and Seferihisar fault (scenario 4 SF), (e and f). The ruptured fault planes are sketched as white boxes and the epicenter for each scenario are marked with a yellow star. To the left (a, c and e) are shown the peak ground acceleration (PGA), the contour colors are from 0-600 cm/s<sup>2</sup>. In the maps to the right (b, d and f) are shown the peak ground velocity (PGV), the contour colors are from 0-80 cm/s.

The ground motion simulations obtained from the scenario earthquakes on Manisa fault (scenario 5A WMF, 5B IMF and 5C EMF) in figure 4, produces very small resulting ground motions in the city of Izmir, although there near the fault art produces peak ground acceleration and velocity values near 300 cm/s<sup>2</sup> and 30 cm/s, respectively. These scenarios

are therefore considered to have the least impact on the city of Izmir compared to the other earthquake scenarios, which have been produced in this study.

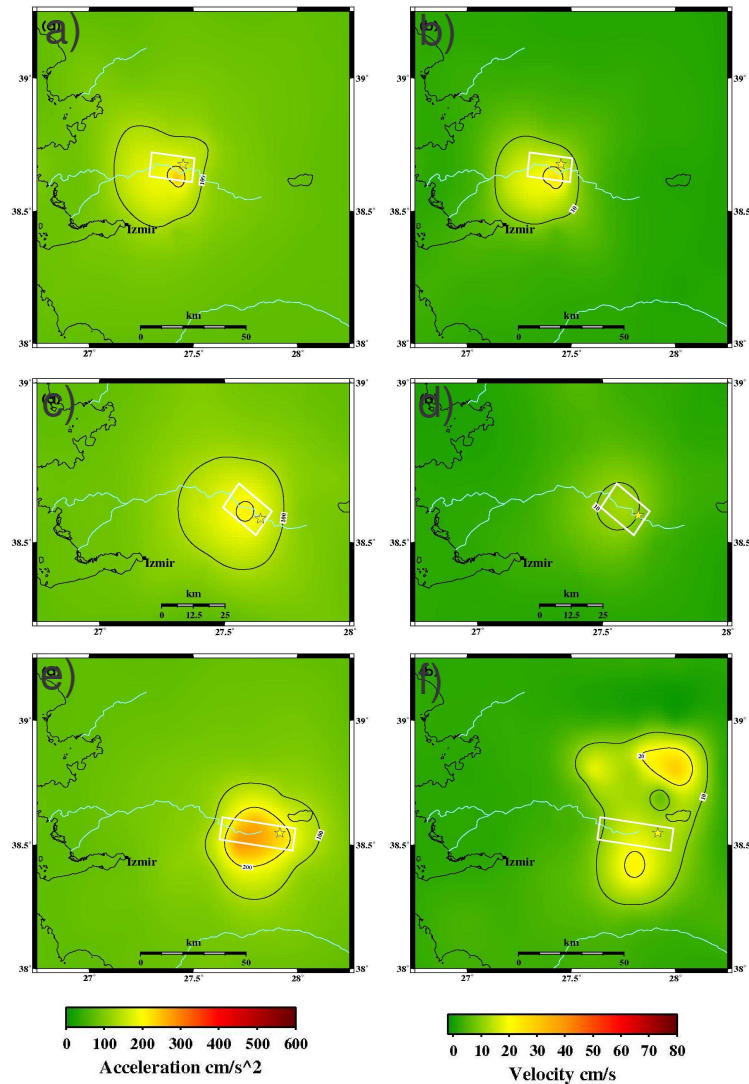


Figure 4: Peak ground motions for the three scenario earthquakes on the Manisa fault. The ruptured fault planes are sketched as white boxes and the epicenter for each scenario are marked with a yellow star. To the left (a, c and e) are shown the peak ground acceleration (PGA), the contour colors are from 0-600  $\text{cm/s}^2$ . In the maps to the right (b, d and f) are shown the peak ground velocity (PGV), the contour colors are from 0-80  $\text{cm/s}$ . The maps in a) and b) shows the peak ground motion distribution for the earthquake scenario on the western segment of the Manisa fault (scenario 5A WMF), c) and d) is for the earthquake scenario of the intermediate segment on the Manisa fault (scenario 5B IMF) and e) and f) is for the earthquake scenario of the eastern segment on the Manisa fault (scenario 5C EMF).

The scope of the ground motion simulation part of this project was to determine which fault ruptures that produce the worst-case scenarios for the city center of Izmir. The damage from an earthquake is not only dependent on the size of the ground motions, but also on the duration of the shaking due to the earthquake. In order to determine the worst-case scenario for the city of Izmir, the peak ground motion values in the center of Izmir for all the scenario earthquakes have been plotted as a function of the signal duration of the simulated waveforms for all scenarios at the station located in the center of Izmir; this is shown in figure 5.

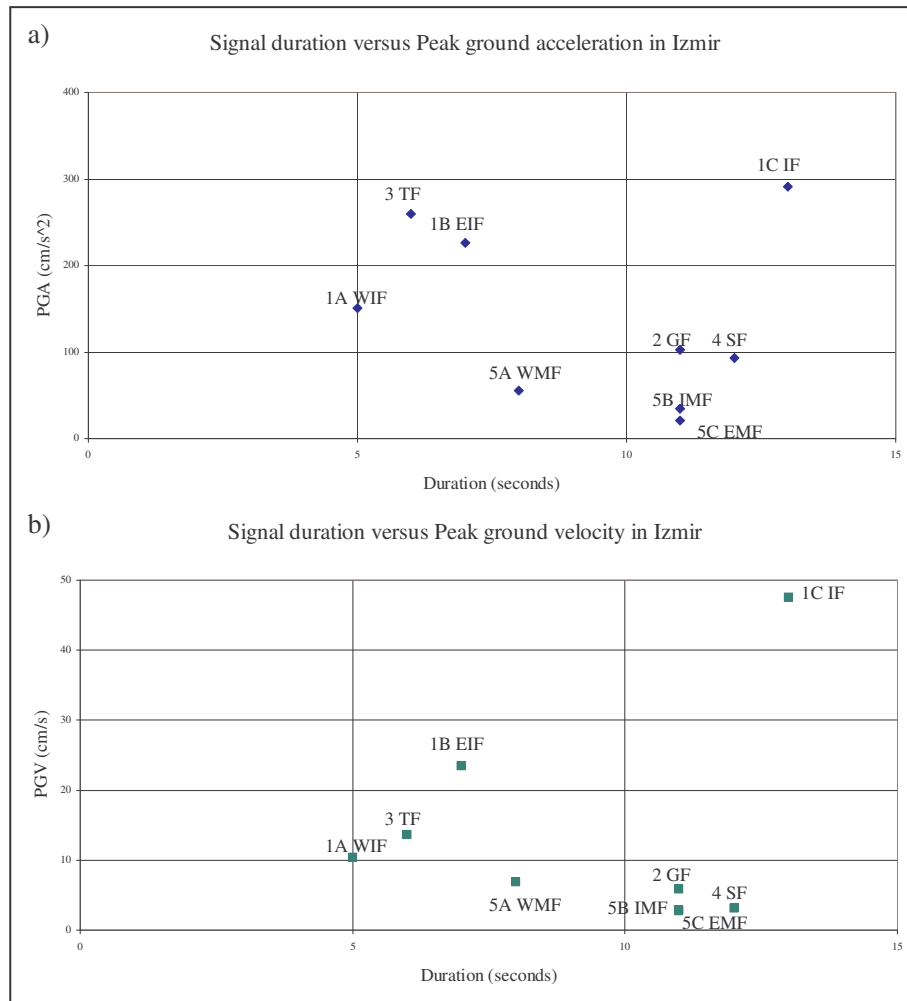


Figure 5: Peak ground motions obtained for the nine earthquake scenarios plotted as a function of the signal duration for a site in the center of Izmir. The earthquake scenarios are identified with their respective abbreviated codes.

Since the peak ground motions for the scenario event on the combined rupture on the Izmir fault (scenario 1C IF) are much higher compared with the signal duration of the other scenarios, this scenario are found to be the worst-case scenario for the city of Izmir. The signal duration is found to be 13 seconds, which is the longest duration obtained in this study. The highest peak ground acceleration and velocity are found to be approximately 290 cm/s<sup>2</sup> and 45 cm/s respectively for the same scenario is much higher than predicted by the general tendency of longer signal duration which is consistent with lower peak ground motions. This tendency is observed for both peak ground accelerations and velocities for the other earthquake scenarios in this study.

#### Attenuation of the ground motion

During the calculations the ground motions based on the earthquake scenarios there have been used a velocity model and an attenuation relation for the area around Izmir, (Akinci et al., 1995; Horasan et al., 2002). In order to check if these values are reasonable, the

simulated peak ground motions have been plotted as a function of the distance to the fault, and then compared to empirical obtained attenuation relations, (Akkar and Bommer, 2007; Ambraseys et al., 1996; Campbell, 1997; Gülkan and Kalkan, 2002; Pankow and Pechmann, 2004; Spudich et al., 1997). The empirical attenuation relations compared to the simulation results are based on both globally and regional datasets.

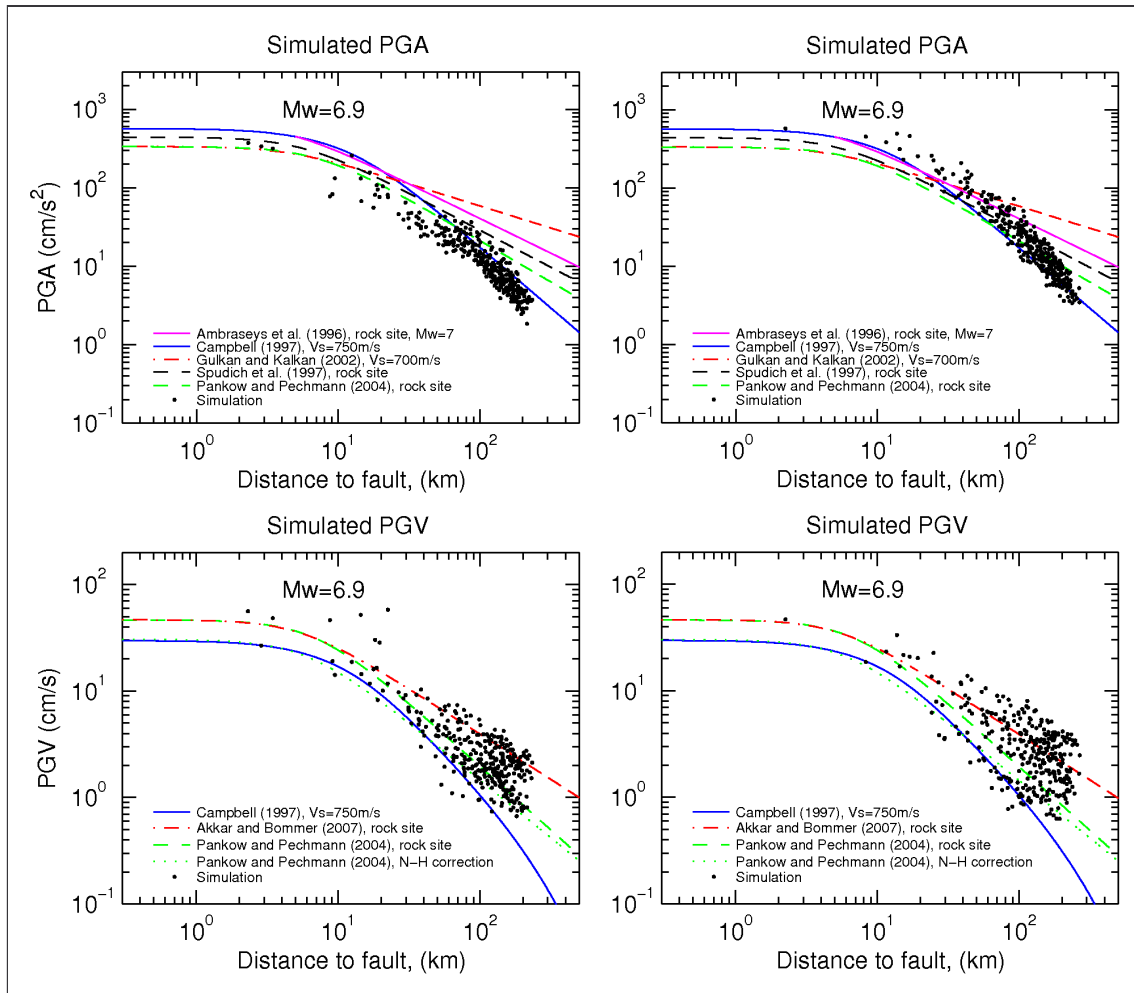


Figure 6: Comparison of simulated (black dots) peak ground acceleration (top) and velocity (bottom) ground motions for the earthquake scenario on the entire Izmir fault (1C IF) (left) and Tuzla fault (3 TF) (right) to predicted by empirical attenuation relations of Ambraseys et al. (1996), Cambel (1997), Gülkan and Kalkan (2002), Spudich et al. (1997), Akkar and Bommer (2007) and Pankow and Pechmann (2004). For the last relation there is in the case of PGV also shown a corrected version by applying the results of Newmark and Hall (1982) for PGV.

There is in figure 6 shown the comparison of the simulated ground motion values, for distances less than 400 kilometers from the faults, on the entire Izmir fault (1C IF) and Tuzla fault (3 TF) with the empirical attenuation relations for the scenarios earthquakes. The two faults are those there are considered to control the hazard in the city of Izmir, and they represent at normal fault and a strike-slip fault respectively. It is seen in figure 6 that the simulated ground motion values are in reasonable agreement with the empirical relations. In the case of the Izmir fault, there is a tendency that the peak ground acceleration (upper left) are lower than predicted by the empirical relations. The shape of the simulated peak ground

acceleration values fit best to the empirical relation of Cambell (1997), blue line. In case of the peak ground velocities (lower left) there is found a larger spread, but the simulated results lies between the values predicted by the upper and lower limits of the empirical attenuation relations. Comparing the simulated ground motions from the earthquake scenario on the Tuzla fault, this is a strike-slip fault, yields higher values than in the case of Izmir fault. It is seen that these results for the peak ground acceleration fits better to the predicted empirical attenuation relations. Figure 6 shows that there seems to be a good agreement between the simulated ground motions and the empirical predictions.

#### Frequency content of ground motion simulations

Since all the ground motion simulations in this study is conducted for bedrock conditions, there has not been taken local site effects into account. There is for the area in the center of Izmir expected to be significant site effects during an earthquake. This is due to that the north-south extension in western Anatolia produces large graben structures, like the origin of Izmir Bay. This basin, which underlies most of the metropolitan area of Izmir, contains accumulated sedimentary deposits. Furthermore, the large river delta of the Gediz river, on the northern part of the Izmir Bay, has brought fluvial deposits to the area, as well as smaller rivers has done on the southern part of the city. Finally the large expansion of the city due to fast development of the metropolitan area has engendered several artificially filled coastal areas.

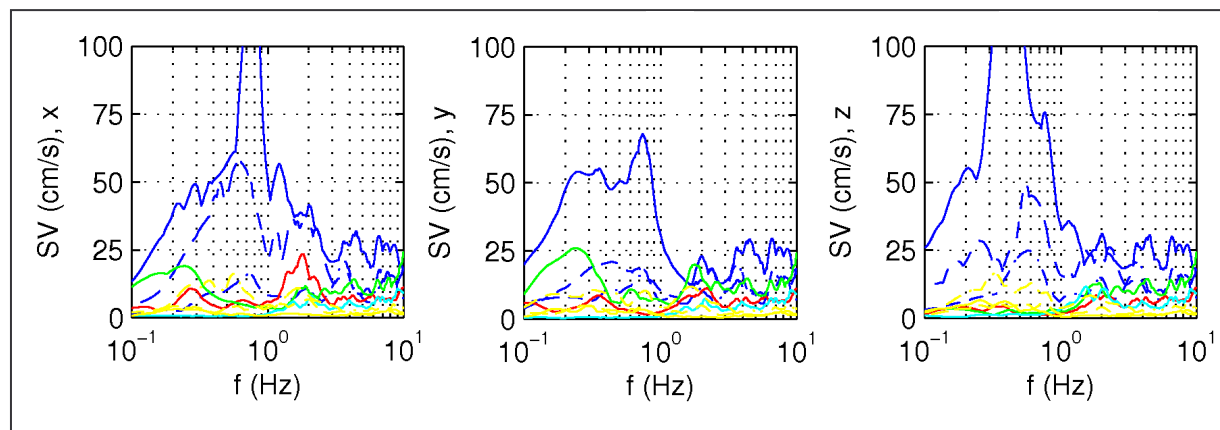


Figure 7: Comparison of the velocity response spectra for all nine earthquake scenarios. Scenario 1A-C (blue), where 1A WIF (- . -), 1B EIF (- -) and 1C IF (a connected line). 2 GF (red), 3 TF (green), 4 SF (light blue), 5A-C (yellow), where 5A WMF (- . -), 5B IMF (- -) and 5C EMF (a connected line). The horizontal components are given as x for east-west and y for north-south, z is the vertical component.

Estimating site effects potential of parts of the area in Izmir is another part of this project, this is among others done by a H/V study, (Nakamura, 1989). In such a study the fundamental frequency are estimated, and in order to compare the values found in the field with the simulated results the simulated velocity response spectra are shown in figure 7. There are produced very low and flat spectral velocity spectra with no major peaks for all scenario

earthquakes except for those for the scenarios on the Izmir fault (1A WIF, 1B EIF and 1C IF). The very high peaks observed for the scenarios on the Izmir fault can be attributed to the short distance from the fault to the site for which the response spectra are calculated.

According to the calculated velocity response spectra, the scenarios on the Izmir fault produce strong peaks in the frequency range on 0.2-1 Hz. In a previously conducted individual study, the fundamental frequency for the area is estimated using the H/V technique, (Nakamura, 1989). This study yields a fundamental frequency in a broad range around 1 Hz, (Atakan, 2005). This leads to the conclusion that there is an overlap in the frequency range and the modeled ground motions are thus expected to amplify significantly in this frequency range.

### **Conclusions**

It can from the ground motion distribution and signal duration be concluded that the worst-case scenario for seismic hazard in the center of Izmir is the scenario where both the western and the eastern part of the Izmir fault (1C IF) ruptures. Also it is observed that there is produces significantly higher ground motions in the center of Izmir for the scenarios conducted on the Izmir and Tuzla faults. Earthquake scenarios on Manisa fault are found to have the least impact on the city of Izmir, and are therefore considered to have be of marginal concern with regard to the hazard in Izmir.

The frequency content of the simulated response spectra is in the same range as the fundamental frequency previously estimated for the area, which suggests a significant site effect potential due to amplification of the simulated seismic waves.

### **Future work on the ground motion simulations**

A realistic seismic hazard assessment is highly dependent upon the understanding of the fault behaviour and consequently a further earthquake hazard assessment will require a detailed fieldwork in the area. The fieldwork should aim at a better understanding of the fault characteristics and possibly also of the fault interactions in order to investigate stress transfer during an earthquake taking the dense location of faults into account.

In the mean time, until such data is available, the very simple fault models used in this study can be changed to be based on more realistic slip-models by using information from previous events, as it is available like the Finite-Source Rupture Model Database, (Mai, 2007). As more information on the input parameters becomes available there needs to be calculated

new earthquake scenarios, especially for the two faults shown in this study to have the largest effect on the hazard in Izmir, Izmir and Tuzla faults.

Since the simulated ground motions are highly dependent on the input parameters, which are hard to constrain, there needs to be conducted a sensitivity study, in order to evaluate the effects of variations in the input parameters. Such a study are suggested to be based on the earthquake scenarios of the rupture along the entire Izmir fault (1C IF) and Tuzla fault (3 TF) which represented the worst-case scenarios for Izmir. Using these two faults in such a study also makes it possible to compare effects of input parameters on normal faults and strike-slip faults, since these fault types are represented by these earthquake scenarios.

The methodology applied in this study for producing a realistic seismic hazard assessment is based on a deterministic approach. However in the area around Izmir, where the earthquake hazard is controlled by several active faults, the seismic hazard estimation should be based on a probabilistic approach. In the currently existing method to assess a probabilistic hazard estimation (PSHA), fault interaction, stress transfer and fault rupture complexity due to fault rupture dynamics and wave propagation is ignored. It is therefore necessary to develop a new technique where hybrid broad-band ground motion simulations from individual rupture scenarios are treated probabilistically.

## References

- Akinci, A., Ibanez, J.M., del Pezzo, E., and Morales, J., 1995, Geometrical spreading and attenuation of Lg waves: a comparison between western Anatolia (Turkey) and southern Spain: *Tectonophysics*, v. **250**, p. 47-60.
- Akkar, S., and Bommer, J.J., 2007, Empirical Prediction Equations for Peak Ground Velocity Derived from Strong-Motion Records from Europe and the Middle East: *Bulletin of the Seismological Society of America*, v. **97**, p. 511-530.
- Ambraseys, N., Simpson, K., and Bommer, J., 1996, Prediction of horizontal response spectra in Europe: *Earthquake engineering and structural dynamics*, v. **25**, p. 371-400.
- Ambraseys, N.N., and Finkel, C.F., 1995, The Seismicity of Turkey and Adjacent Areas, A Historical Review, 1500-1800: Istanbul, Muhittin Salih EREN.
- Atakan, A., 2005, Mikrotremor ölçümleri ve mühendislik uygulamaları *Chamber of Geophysical Engineers: Izmir, Turkey*.
- Benetatos, C., Kiratzi, A., Ganas, A., Ziazia, M., Plessa, A., and Drakatos, G., 2006, Strike-slip motions in the Gulf of Sigacik (western Turkey): Properties of the 17 October 2005 earthquake seismic sequence: *Tectonophysics*, v. **426**, p. 263-279.
- Campbell, K.W., 1997, Empirical Near-Source Attenuation Relationships for Horizontal and Vertical Components of Peak Ground Acceleration, Peak Ground Velocity, and Pseudo-Absolute Acceleration Response Spectra: *Seismological Research Letters*, v. **68**, p. 154-179.
- Emre, Ö., Dogan, A., Özalp, S., and Yildirim, C., 2005a, 17 Ekim 2005 Sigacik (Izmir) Depremleri Ön Değerlendirme Raporu: **Ankara, Maden Tetkik ve Arama Genel Müdürlüğü**, p. 6.

- Emre, Ö., Özalp, S., Dogan, A., Özaksoy, V., Yildirim, C., and Göktas, F., 2005b, Izmir Yakın Çevresinin Diri Faylari Ve Deprem Potansiyelleri, *Maden Tetkik ve Arama, MTA*, p. 80.
- Gülkan, P., and Kalkan, E., 2002, Attenuation modeling of recent earthquakes in Turkey: *Journal of Seismology*, v. **6**, p. 397-409.
- Horasan, G., Gulen, L., Pinar, A., Kalafat, D., Ozel, N., Kuleli, H.S., and Isikara, A.M., 2002, Lithospheric Structure of the Marmara and Aegean Regions, Western Turkey: *Bulletin of the Seismological Society of America*, v. **92**, p. 322-329.
- Larson, E., 2006, Global CMT Catalog search, *G. Ekström and N. Nettles*.
- Mai, M., 2007, SRCMOD: a database of finite-source rupture models, <http://www.seismo.ethz.ch/srcmod/> *Schweizerischer Erdbebendienst (SED) Swiss Seismological Service*.
- Nakamura, Y., 1989, A method for dynamic characteristics estimation of subsurface using microtremor on the ground surface: *Quarterly Report of RTRI*, v. **30**, p. 25-33.
- Pankow, K.L., and Pechmann, J.C., 2004, The SEA99 Ground-Motion Predictive Relations for Extensional Tectonic Regimes: Revisions and a New Peak Ground Velocity Relation: *Bulletin of the Seismological Society of America*, v. **94**, p. 341-348.
- Papazachos, B., and Papazachou, C., 1997, The Earthquakes of Greece: **Thessaloniki**, *Technical books Edition*.
- Pulido, N., and Kubo, T., 2004, Near-fault strong motion complexity of the 2000 Tottori earthquake (Japan) from a broadband source asperity model: *Tectonophysics*, v. **390**, p. 177-192.
- Pulido, N., Ojeda, A., Atakan, A., and Kubo, T., 2004, Strong ground motion estimation in the Sea of Marmara region (Turkey) based on a scenario earthquake: *Tectonophysics*, v. **391**, p. 357-374.
- Spudich, P., Fletcher, J.B., Hellweg, M., Boatwright, J., Sullivan, C., Joyner, W.B., Hanks, T.C., Boore, D.M., McGarr, A., Baker, L.M., and Lindh, A.G., 1997, SEA96 - A New Predictive Relation for Earthquake Ground Motions in Extensional Tectonic Regimes: *Seismological Research Letters*, v. **68**, p. 190-198.
- Sørensen, M.B., Atakan, K., and Pulido, N., 2007, Simulated Strong Ground Motions for the Great M 9.3 Sumatra-Andaman Earthquake of 26 December 2004: *Bulletin of the Seismological Society of America*, v. **97**, p. S139-151.